UNIVERSITY OF OXFORD
OCCAM
OXFORD CENTRE FOR COLLABORATIVE APPLIED MATHEMATICS

Singular inextensible limit in the vibrations of post-buckled rods: analytical derivation and role of boundary conditions

by

Sébastien Neukirch
Alain Goriely
Oliver Thomas

OCCAM Preprint Number 13/32

Elsevier Editorial System(tm) for Journal of Sound and Vibration

Manuscript Draft

Manuscript Number:

Title: Singular inextensible limit in the vibrations of post-buckled rods: analytical derivation and role of boundary conditions

Article Type: Full Length Article

Section/Category: I Nonlinear aspects of sound and vibration

Keywords: Vibrations
Kirchhoff elastic rods
Buckling
Bifurcation

Corresponding Author: Dr. sebastien neukirch,

Corresponding Author's Institution:

First Author: sebastien neukirch

Order of Authors: sebastien neukirch; alain goriely; olivier thomas

Abstract: In-plane vibrations of an elastic rod clamped at both extremities are studied. The rod is modeled as an extensible planar Kirchhoff elastic rod under large displacements and rotations. Equilibrium configurations and vibrations around these configurations are computed analytically in the incipient post-buckling regime. Of particular interest is the variation of the first mode frequency as the load is increased through the buckling threshold. The loading type is found to have a crucial importance as the first mode frequency is shown to behave singularly in the zero thickness limit in case of prescribed axial displacement, whereas a regular behavior is found in the case of prescribed axial load.

dear editor,

the present paper could be seen as a sequel to:

S. Neukirch, J. Frelat, A. Goriely, and C. Maurini
Vibrations of post-buckled rods: The singular inextensible limit
Journal of sound and Vibration, 331 (2012) 704-720

We present analytical calculations where the source of the singular behavior in the vibration of post-buckled beams is clearly identified.

We also show analytically that boundary conditions play a crucial role in this singular behavior: the singular behavior is present in the case of prescribed axial displacement and vanishes in the case of prescribed axial load.

Finally we also show that in this post-buckling regime the first mode vibration frequency also strongly depends on the loading, being 4 times higher in the case of prescribed axial displacement (compared to prescribed axial load).

Singular inextensible limit in the vibrations of post-buckled rods: analytical derivation and role of boundary conditions

Sébastien Neukirch[1a,b], Alain Goriely[c], Olivier Thomas[d]

[a]CNRS, UMR 7190, Institut Jean Le Rond d'Alembert, F-75005 Paris, France.
[b]UPMC Univ Paris 06, UMR 7190, Institut Jean Le Rond d'Alembert, F-75005 Paris, France.
[c]Oxford Centre for Collaborative Applied Mathematics (OCCAM), Oxford University, U.K.
[d]Laboratoire des Sciences de l'Information et des Systèmes, ENSAM, Lille, France

Abstract

In-plane vibrations of an elastic rod clamped at both extremities are studied. The rod is modeled as an extensible planar Kirchhoff elastic rod under large displacements and rotations. Equilibrium configurations and vibrations around these configurations are computed analytically in the incipient post-buckling regime. Of particular interest is the variation of the first mode frequency as the load is increased through the buckling threshold. The loading type is found to have a crucial importance as the first mode frequency is shown to behave singularly in the zero thickness limit in case of prescribed axial displacement, whereas a regular behavior is found in the case of prescribed axial load.

Keywords: Vibrations, Kirchhoff elastic rods, Buckling, Bifurcation.

1. Introduction

External loads and boundary conditions are known to play a key role in the statics and dynamics of elastic structures. In the analysis of vibrations of a string or a rod, external loads have a direct influence on the response of the system, e.g. tension in a string raises its natural frequency whereas compression in a rod lowers its natural frequency. Nonlinear effects become important when external loads not only change the vibration response of the rod but also alter its overall stability through buckling. Several studies have investigated dynamical responses of post-buckled elastic rods [1, 2]. Vibrations and resonance are also used to destabilize buckled beams [3, 4]. In a classical buckling experiment with clamped boundary conditions there are two

[1]corresponding author: email sebastien.neukirch@upmc.fr / Tel +33 1 44 27 87 13

ways to apply the loading: the distance between the two ends may be imposed (and we refer to this situation as prescribed axial displacement or rigid loading), or the axial force pushing the two ends together may be imposed (and we refer to this situation as prescribed axial load or dead loading). In fact due to the intrinsic elasticity of any loading device, one is never exactly in a pure dead or rigid loading situation [5]. For equilibrium the response of the system is the same under both loadings, axial force and axial displacement being conjugate variables in the energy of the system. But as soon as stability and vibrations are considered the response of the system strongly depends on the loading type, with rigid loading setups typically being more stable that dead loading ones [6].

Here, we consider the problem of in-plane vibrations of a post-buckled Kirchhoff extensible unshearable elastic rod with clamped boundary conditions under rigid and dead loadings. First, we study the post-buckled equilibrium configurations of the rod. We then focus on the small-amplitude vibrations around the equilibrium state and look how the first mode frequency evolves as the rod goes into the post-buckling regime, comparing the rigid and dead loading cases.

We recall Kirchhoff model for elastic rods in Section 2 and derive vibrations equations in Section 3. We then compute analytically the incipient post-buckling equilibrium solution in Section 4 and the first mode vibration around this equilibrium solution in Section 5, in the rigid loading case (Section 5.1) and in the dead loading case (Section 5.2). Discussion (Section 6) and conclusion (Section 7) follow.

2. Model

We consider an elastic rod with a rectangular cross section of width b and thickness h, total length L and arc length S in its unstressed reference state. In this state the rod lies along the $\boldsymbol{e_x}$ axis, from the origin $O = (0, 0, 0)$ to the point at $(L, 0, 0)$. The position vector of the center of the rod cross section is noted $\boldsymbol{R}(S)$ and we have $\boldsymbol{R}(0) = (0, 0, 0)$ and $\boldsymbol{R}(L) = (L, 0, 0)$ in the reference state.

Kinematics

We use the special Cosserat theory of rods [7] where the rod can suffer bending and extension, but no shear. We work under the assumption that the rod cross section remains planar (and rectangular) as the rod deforms and use a set of three Cosserat directors $(\boldsymbol{d_1}(S), \boldsymbol{d_2}(S), \boldsymbol{d_3}(S))$

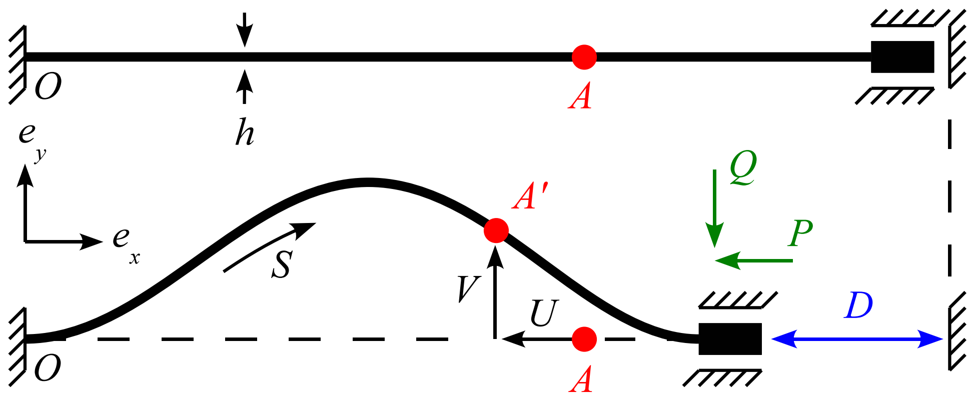

Figure 1: Clamped-clamped rod buckled in the (x, y) plane. Either the end-shortening D or axial load P is controlled. The point A in the reference configuration moves to point A' in the deformed configuration, introducing horizontal $U \leq 0$ and vertical V displacements. The origin O is at the left end of the rod.

embedded in each cross section: $\boldsymbol{d_1}$ is perpendicular to the section plane, $\boldsymbol{d_2}$ is along the small span (of length h) of the section, and $\boldsymbol{d_3}$ is along the wide span (of length b) of the section. In the undeformed state, $\boldsymbol{d_1}(S) \equiv \boldsymbol{e_x}$, $\boldsymbol{d_2}(S) \equiv \boldsymbol{e_y}$, and $\boldsymbol{d_3}(S) \equiv \boldsymbol{e_z}$. We only consider deformed states that are (i) planar (where the rod center line $\boldsymbol{R}(S)$ lies in the (x, y) plane, the rod being bent along its small span h), and (ii) twist-less (where the director $\boldsymbol{d_3}(S) \equiv \boldsymbol{e_z}$). Note that in the presence of extension, S may no longer be the arc length of the curve $\boldsymbol{R}(S)$ in the deformed state. We introduce the extension $e(S)$ with:

$$\boldsymbol{R}'(S) \stackrel{\text{def}}{=} \mathrm{d}\boldsymbol{R}/\mathrm{d}S = (1 + e(S))\, \boldsymbol{d_1}\,. \tag{1}$$

In the absence of extension ($e = 0$) the director $\boldsymbol{d_1}$ is the unit tangent to the centerline $\boldsymbol{R}(S) = (X(S), Y(S), Z(S))$. We introduce the angle $\theta(S)$ to parametrize the rotation of the $(\boldsymbol{d_1}, \boldsymbol{d_2})$ frame around the $\boldsymbol{e_z} = \boldsymbol{d_3}$ axis:

$$\boldsymbol{d_1}(S) = \begin{pmatrix} \cos\theta(S) \\ \sin\theta(S) \\ 0 \end{pmatrix}_{\boldsymbol{e_x},\boldsymbol{e_y},\boldsymbol{e_z}} \quad \text{and} \quad \boldsymbol{d_2}(S) = \begin{pmatrix} -\sin\theta(S) \\ \cos\theta(S) \\ 0 \end{pmatrix}_{\boldsymbol{e_x},\boldsymbol{e_y},\boldsymbol{e_z}}\,. \tag{2}$$

Dynamics

We use Kirchhoff dynamical equations for elastic rods [7], where the stresses in the section are averaged to yield an internal force $\boldsymbol{N}(S)$ and an internal moment $\boldsymbol{M}(S)$. These internal forces and moments are the loads exerted on the section at S by the part of the rod at $\tilde{S} > S$. In the absence of body force and couple, the linear and angular momentum balance read

$$\begin{aligned} \boldsymbol{N}'(S,T) &= \rho A\, \ddot{\boldsymbol{R}}(S,T), && (3)\\ \boldsymbol{M}'(S,T) + \boldsymbol{R}'(S,T)\times \boldsymbol{N}(S,T) &= \rho I\, \ddot{\theta}(S,T)\,, && (4) \end{aligned}$$

where $(\ )' \stackrel{\text{def}}{=} \partial/\partial S$, $(\dot{\ }) \stackrel{\text{def}}{=} \partial/\partial T$, T is time, ρ the density of the material, A the area of the cross section (in the present case $A = hb$), and I the second moment of area of the cross section (in the present case $I = h^3 b/12$). As we are only interested in low frequencies we neglect the rotational inertia, that is the left-hand side of (4) will be zero.

Constitutive law

We use the standard linear constitutive relationship relating the bending strain $\kappa(S) \stackrel{\text{def}}{=} \theta'(S)$ to the bending moment $M_3 \stackrel{\text{def}}{=} \boldsymbol{M}\cdot\boldsymbol{d_3}$:

$$M_3 = E\, I\, \kappa, \tag{5}$$

where E is Young's modulus. Note that κ is not the curvature in general. The extension constitutive law relates the tension $\boldsymbol{N}\cdot\boldsymbol{d_1}$ to the extension e:

$$N_x \cos\theta + N_y \sin\theta = EA\, e \tag{6}$$

Equations in component form

In the planar case considered here, we have $Z(S,T) \equiv 0$, $N_z(S,T) \equiv 0$, $M_x(S,T) \equiv 0$, and $M_y(S,T) \equiv 0\ \forall(S,T)$ and the equations for the six remaining unknowns are

$$\begin{aligned} X' &= (1+e)\cos\theta, && \text{(7a)}\\ Y' &= (1+e)\sin\theta, && \text{(7b)}\\ \theta' &= M/(EI), && \text{(7c)}\\ M' &= (1+e)\,(N_x \sin\theta - N_y\cos\theta), && \text{(7d)}\\ N_x' &= \rho h b\, \ddot{X}, && \text{(7e)}\\ N_y' &= \rho h b\, \ddot{Y}, && \text{(7f)} \end{aligned}$$

where $M = M_z = M_3$ and the extension e is given by Eqs (6).

Dimensionless variables

We scale all lengths with L, time with $\tau \overset{\text{def}}{=} L^2 \sqrt{\rho h b/(EI)}$, forces with EI/L^2, and moments with EI/L. This naturally introduces a parameter

$$\eta \overset{\text{def}}{=} \frac{I}{AL^2} = \frac{1}{12}\left(\frac{h}{L}\right)^2 , \tag{8}$$

which takes small values in the present case of slender rods. Dimensionless variables will be written lowercase, e.g. $s \overset{\text{def}}{=} S/L$, $x \overset{\text{def}}{=} X/L$, or $m \overset{\text{def}}{=} ML/(EI)$. The constitutive relation (6) reads:

$$e = \eta\,(n_x \cos\theta + n_y \sin\theta)\,. \tag{9}$$

The case $\eta > 0$ corresponds to extensible rods, the case $\eta = 0$ to inextensible rods. The particular case $\eta = 0$ has been studied in detail in [8] and we will assume for the present study that $\eta \neq 0$ and only briefly comment on the inextensible case.

3. Small-amplitude vibrations around equilibrium configurations

The systems of equations (7) in dimensionless form reads

$$x'(s,t) = \Big(1 + \eta\, n_x \cos\theta + \eta\, n_y \sin\theta\Big) \cos\theta\,, \tag{10a}$$

$$y'(s,t) = \Big(1 + \eta\, n_x \cos\theta + \eta\, n_y \sin\theta\Big) \sin\theta\,, \tag{10b}$$

$$\theta'(s,t) = m\,, \tag{10c}$$

$$m'(s,t) = \Big(1 + \eta\, n_x \cos\theta + \eta\, n_y \sin\theta\Big) \Big(n_x \sin\theta - n_y \cos\theta\Big)\,, \tag{10d}$$

$$n_x'(s,t) = \ddot{x}\,, \tag{10e}$$

$$n_y'(s,t) = \ddot{y}\,. \tag{10f}$$

We consider a rod subject to clamped-clamped boundary conditions:

$$x(0,t) = 0 \tag{11a}$$

$$y(0,t) = 0 \qquad y(1,t) = 0\,, \tag{11b}$$

$$\theta(0,t) = 0 \qquad \theta(1,t) = 0\,. \tag{11c}$$

The rod is subject to either dead or rigid loading. In the rigid loading setup we control the end-shortening d, that is we impose the additional boundary condition

$$x(1,t) = 1 - d\,, \tag{12}$$

and the axial load $p(t) = -n_x(1,t)$ is unknown and varying with time. In the dead loading case, a constant axial load p is imposed, replacing (12) by

$$n_x(1,t) = p\,, \tag{13}$$

while the end-shortening $d(t)$ becomes a time-varying unknown. Note that in both cases the transverse displacement $y(1,t) = 0$ being fixed, the shear load $q(t) = n_y(1,t)$ is a time-varying unknown. For a given ratio η we first look for the equilibrium configuration (x_e, y_e, θ_e, m_e, n_{xe}, n_{ye}), solution to (10) with $\ddot{x}_e = 0$ and $\ddot{y}_e = 0$, and then we look for small amplitude vibrations around the equilibrium configuration, that is we set

$$\begin{aligned}
x(s,t) &= x_e(s) + \delta\,\overline{x}(s)\,\mathrm{e}^{\mathrm{i}\omega t}, && \text{(14a)}\\
y(s,t) &= y_e(s) + \delta\,\overline{y}(s)\,\mathrm{e}^{\mathrm{i}\omega t}, && \text{(14b)}\\
\theta(s,t) &= \theta_e(s) + \delta\,\overline{\theta}(s)\,\mathrm{e}^{\mathrm{i}\omega t}, && \text{(14c)}\\
m(s,t) &= m_e(s) + \delta\,\overline{m}(s)\,\mathrm{e}^{\mathrm{i}\omega t}, && \text{(14d)}\\
n_x(s,t) &= n_{xe}(s) + \delta\,\overline{n}_x(s)\,\mathrm{e}^{\mathrm{i}\omega t}, && \text{(14e)}\\
n_y(s,t) &= n_{ye}(s) + \delta\,\overline{n}_y(s)\,\mathrm{e}^{\mathrm{i}\omega t}, && \text{(14f)}
\end{aligned}$$

where $\delta \ll 1$ is a small amplitude parameter, and ω is the frequency of the vibration. Inserting (14) into (10) and keeping only linear terms in δ, we obtain equations for the spatial modes $(\overline{x}, \overline{y}, \overline{\theta}, \overline{m}, \overline{n}_x, \overline{n}_y)$:

$$\begin{aligned}
\overline{x}'(s) &= -\left(1 + \eta\, n_{xe}\cos\theta_e + \eta\, n_{ye}\sin\theta_e\right)\overline{\theta}\,\sin\theta_e + \overline{e}\,\cos\theta_e\,, && \text{(15a)}\\
\overline{y}'(s) &= \left(1 + \eta\, n_{xe}\cos\theta_e + \eta\, n_{ye}\sin\theta_e\right)\overline{\theta}\,\cos\theta_e + \overline{e}\,\sin\theta_e\,, && \text{(15b)}\\
\overline{\theta}'(s) &= \overline{m}\,, && \text{(15c)}\\
\overline{m}'(s) &= \left(1 + \eta\, n_{xe}\cos\theta_e + \eta\, n_{ye}\sin\theta_e\right)\left(\overline{n}_x\sin\theta_e - \overline{n}_y\cos\theta_e + \overline{\theta}\left[(n_{xe}\cos\theta_e + n_{ye}\sin\theta_e\right]\right)\\
&\quad + \overline{e}\left(n_{xe}\sin\theta_e - n_{ye}\cos\theta_e\right)\,, && \text{(15d)}\\
\overline{n}_x'(s) &= -\omega^2\,\overline{x}\,, && \text{(15e)}\\
\overline{n}_y'(s) &= -\omega^2\,\overline{y}\,, && \text{(15f)}
\end{aligned}$$

where we introduced

$$\overline{e} = \eta\left(\overline{n}_x\cos\theta_e + \overline{n}_y\sin\theta_e - \overline{\theta}\left[n_{xe}\sin\theta_e - n_{ye}\cos\theta_e\right]\right). \tag{16}$$

The boundary conditions on the spatial modes are

$$\overline{x}(0) = 0 \qquad \star \tag{17a}$$

$$\overline{y}(0) = 0 \qquad \overline{y}(1) = 0\,, \tag{17b}$$

$$\overline{\theta}(0) = 0 \qquad \overline{\theta}(1) = 0\,. \tag{17c}$$

with $\star$ replaced by $\overline{x}(1) = 0$ in the rigid loading case, and by $\overline{n}_x(1) = 0$ in the dead loading case. The 6D system (15) with the six boundary conditions (17) is a well-defined generalized eigenvalue problem, with eigenvalue ω. For computational purpose, we normalize the linear solution of this problem by imposing the condition

$$\overline{m}^2(0) + \overline{n}_x^2(0) + \overline{n}_y^2(0) = 1. \tag{18}$$

4. Post-buckled equilibrium configurations

In order to obtain the vibrations in the post-buckling regime we first have to calculate the post-buckled equilibrium solution. As the end-shortening or the axial load is increased from zero, the rod first experiences axial compression until eventually buckling is reached and flexural deformations kick in. We have shown in [8] that the buckling threshold $p^\star$ for an extensible rod with clamped boundary conditions is given by $p^\star\,(1 - \eta\, p^\star) = 4\pi^2$, that is

$$p^\star = \frac{1 - \sqrt{1 - 16\pi^2\eta}}{2\eta} = 4\pi^2 + 16\pi^4\eta + O\left(\eta^2\right)\,. \tag{19}$$

We now study the equilibrium solutions in the post-buckling regime. Equilibrium equations are obtained by setting $\ddot{x} = 0$ and $\ddot{y} = 0$ in system (10). At equilibrium the internal force vector is found to be uniform along the rod and we write: $n_{xe}(s) = -p_e$ and $n_{ye}(s) = -q_e\ \forall s$. System (10) is then reduced to

$$x_e' = (1 - \eta p_e \cos\theta_e - \eta q_e \sin\theta_e)\cos\theta_e \quad \text{with} \quad x_e(0) = 0\,, \tag{20a}$$

$$y_e' = (1 - \eta p_e \cos\theta_e - \eta q_e \sin\theta_e)\sin\theta_e \quad \text{with} \quad y_e(0) = 0 = y_e(1)\,, \tag{20b}$$

$$\theta_e'' = (1 - \eta p_e \cos\theta_e - \eta q_e \sin\theta_e)\,(-p_e \sin\theta_e + q_e\cos\theta_e) \quad \text{with} \quad \theta_e(0) = 0 = \theta_e(1)\,. \tag{20c}$$

For the first buckling mode, we are looking for an equilibrium shape whose curvature is symmetric about the middle point $s = 1/2$, hence we require $m_e'(s - 1/2)$ to be an odd function. From (10d) the function $n_{ye}(s - 1/2)$ has to be odd as well, eventually imposing $q_e = 0$.

We address the behavior of the solutions after, but close to, buckling. Therefore, we expand the variables in powers of ϵ, a small parameter measuring the distance from buckling:

$$\theta_e(s) = \epsilon\theta_1(s) + \epsilon^2\theta_2(s) + \epsilon^3\theta_3(s) + O\left(\epsilon^4\right), \tag{21a}$$

$$x_e(s) = x_0(s) + \epsilon x_1(s) + \epsilon^2 x_2(s) + \epsilon^3 x_3(s) + O\left(\epsilon^4\right), \tag{21b}$$

$$y_e(s) = \epsilon y_1(s) + \epsilon^2 y_2(s) + \epsilon^3 y_3(s) + O\left(\epsilon^4\right), \tag{21c}$$

$$p_e = p_0 + \epsilon p_1 + \epsilon^2 p_2 + \epsilon^3 p_3 + O\left(\epsilon^4\right). \tag{21d}$$

We substitute these expansions in the equilibrium equations (20), which have to be satisfied to all orders in ϵ. The solution up to order 3 reads:

$$\theta_e(s) = \epsilon \sin 2\pi s + \epsilon^3 \frac{16\pi^2 - 3\,p_0}{192\pi^2} \cos^2(2\pi s)\sin(2\pi s) + O\left(\epsilon^4\right), \tag{22a}$$

$$x_e(s) = s(1-\eta p_0) - \epsilon^2 \frac{(1-2\eta p_0)^2\,(4\pi s - \sin 4\pi s) + 2\pi s\,\eta\left(16\pi^2 - 3p_0\right)}{16\pi(1-2\eta p_0)} + O\left(\epsilon^4\right), \tag{22b}$$

$$y_e(s) = \frac{2\pi\epsilon}{p_0}(1-\cos 2\pi s) - \frac{\epsilon^3 \sin^2(\pi s)}{96\pi(1-2\eta p_0)}\left(c_u + c_v\cos(2\pi s) + c_w\cos(4\pi s)\right) + O\left(\epsilon^4\right), \tag{22c}$$

$$p_e = p_0 + \epsilon^2 \frac{16\pi^2 - 3p_0}{8(1-2\eta p_0)} + O\left(\epsilon^4\right), \text{ with } p_0 = \frac{1-\sqrt{1-16\pi^2\eta}}{2\eta}. \tag{22d}$$

where $c_u = 7 - 22\eta p_0 - 32\eta\pi^2$, $c_v = -6\,(1 + 2\eta p_0 - 32\eta\pi^2)$, and $c_w = -3 - 6\eta p_0 + 96\eta\pi^2$. From (9) we recover the extension:

$$e_e(s) = -\eta p_0 - \eta\left(\frac{16\pi^2 - 3p_0}{8(1-2\eta p_0)} - \frac{1}{2}p_0\sin^2(2\pi s)\right)\epsilon^2 + O\left(\epsilon^4\right). \tag{23}$$

Equations (20) were solved in the absence of any condition on the axial loading, and consequently solutions (22) is valid for both dead and rigid loadings. From (22b) and (22d) we eliminate ϵ and write the relation:

$$d_e - \eta p_0 = \frac{2 - 3\eta p_0 - 16\eta\pi^2}{16\pi^2 - 3p_0}(p_e - p_0) + O\left((p_e - p_0)^2\right) \tag{24}$$

between the axial load p_e and the axial displacement $d_e = 1 - x_e(1)$. In dead loading the load p_e is prescribed and the resulting end-shortening d_e is computed form (24). Respectively in rigid loading the end-shortening d_e is prescribed and the resulting axial load p_e is computed for the same equation (24). We therefore see that the equilibrium solution does not depend on the loading type.

5. Vibrations around post-buckled equilibrium configurations

We expand all modal variables $(\overline{x}, \overline{y}, \overline{\theta}, \overline{m}, \overline{n}_x, \overline{n}_y)$ and the frequency ω in powers of ϵ. For instance we have $\omega = \omega_0 + \epsilon\omega_1 + \epsilon^2\omega_2 + \epsilon^3\omega_3 + O(\epsilon^4)$, and so on. We restrict the study to the fundamental frequency which is zero at buckling; consequently we set $\omega_0 = 0$. We solve equations (15) with boundary conditions (17), using the equilibrium solution (22). Contrary to the equilibrium solution we show that the vibration solution strongly depends on the loading type.

5.1. Vibrations in the rigid loading case

In the rigid loading case we use the boundary condition $\overline{x}(1) = 0$ in (17). To order ϵ^0 we solve:

$$\begin{aligned} \overline{x}_0' &= \eta\,\overline{n}_{x0} \quad \text{with} \quad \overline{x}_0(0) = 0 = \overline{x}_0(1)\,, && (25a)\\ \overline{n}_{x0}' &= 0\,, && (25b)\\ \overline{y}_0'''' + 4\pi^2\overline{y}_0'' &= 0 \quad \text{with} \quad \overline{y}_0(0) = \overline{y}_0(1) = \overline{y}_0'(0) = \overline{y}_0'(1) = 0\,. && (25c) \end{aligned}$$

The first two equations describe the longitudinal mode and are decoupled from the third one which is associated with the transverse mode. The solution is:

$$\begin{aligned} \overline{x}_0(s) &= 0\,, && (26a)\\ \overline{n}_{x0}(s) &= 0\,, && (26b)\\ \overline{y}_0(s) &= A_0(1 - \cos 2\pi s)\,. && (26c) \end{aligned}$$

where A_0 is the linear small amplitude of the vibration mode. To ordre ϵ^1 we have to solve:

$$\begin{aligned} \overline{x}_1' &= \eta\,\overline{n}_{x1} - 2\pi A_0 \frac{1 - 2\eta p_0}{1 - \eta p_0} \sin^2(2\pi s) \quad \text{with} \quad \overline{x}_1(0) = 0 = \overline{x}_1(1)\,, && (27a)\\ \overline{n}_{x1}' &= 0\,, && (27b)\\ \overline{y}_1'''' + 4\pi^2\overline{y}_1'' &= 0 \quad \text{with} \quad \overline{y}_1(0) = \overline{y}_1(1) = \overline{y}_1'(0) = \overline{y}_1'(1) = 0\,. && (27c) \end{aligned}$$

The transverse mode solution

$$\overline{y}_1(s) = A_1(1 - \cos 2\pi s) \qquad (28)$$

is a multiple of $\overline{y}_0(s)$, and we set $A_1 = 0$ without loss of generality (this amounts to redefining ϵ, see also [9]). For the longitudinal mode, (27b) requires $\overline{n}_{x1}(s)$ to be constant and we note

$\bar{n}_{x1}(s) = c_{nx1}$. We then integrate (27a) and ask for the boundary condition $\bar{x}_1(1) = 0$ to be met. This yields:

$$\eta\, c_{nx1}\,(1-\eta p_0) - \pi\, A_0\,(1-2\eta p_0) = 0\,, \tag{29}$$

which typically determines c_{nx1}. We nevertheless remark that in the inextensional case $\eta = 0$ one concludes that $A_0 = 0$, which eventually prevents the $\omega_0 = 0$ mode to exist, see [8] for more details. In the extensional case we have:

$$\begin{aligned} \bar{x}_1(s) &= A_0\,\frac{1-2\eta p_0}{1-\eta p_0}\,\frac{\sin 4\pi s}{4}\,, && (30a)\\ \bar{n}_{x1}(s) &= A_0\,\frac{1-2\eta p_0}{1-\eta p_0}\,\frac{\pi}{\eta}\,. && (30b) \end{aligned}$$

We note that the $1/\eta$ singularity appearing in (30b) eventually leads to the frequency ω to be singular as $\eta \to 0$, see (37). This singularity has its roots in the boundary condition $\bar{x}_1(1) = 0$, that is prescribed axial displacement. We show in Section 5.2 that in the case of prescribed axial load no such singularity is present. To ordre ϵ^2, longitudinal mode equations are:

$$\begin{aligned} \bar{x}_2' &= \eta\,\bar{n}_{x2} \quad \text{with} \quad \bar{x}_2(0) = 0 = \bar{x}_2(1)\,, && (31a)\\ \bar{n}_{x2}' &= 0\,. && (31b) \end{aligned}$$

and their solution is:

$$\begin{aligned} \bar{x}_2(s) &= 0\,, && (32a)\\ \bar{n}_{x2}(s) &= 0\,. && (32b) \end{aligned}$$

For the tranversal mode, equations are

$$\bar{y}_2'''' + 4\pi^2 \bar{y}_2'' = c_\alpha \cos 6\pi s + c_\beta \cos 2\pi s + c_\gamma \quad \text{with} \quad \bar{y}_2(0) = \bar{y}_2(1) = \bar{y}_2'(0) = \bar{y}_2'(1) = 0\,, \tag{33}$$

with

$$\begin{aligned} c_\alpha &= -54\pi^4 A_0\,\frac{1-4\eta p_0}{1-\eta p_0}\,, && (34a)\\ c_\beta &= \frac{A_0}{\eta\,[1-\eta\,(8\pi^2+p_0)]}\,\Big\{2\pi^2\Big[1-\eta\Big(22\pi^2+p_0-20\pi^2\eta p_0-64\pi^4\eta\Big)\Big] \\ &\qquad -\eta\omega_1^2\Big[1-\eta\Big(16\pi^2+p_0-12\pi^2\eta p_0-32\pi^4\eta\Big)\Big]\Big\}\,, && (34b)\\ c_\gamma &= A_0\,\omega_1^2\,\Big[1-\eta\,\Big(4\pi^2+p_0\Big)\Big]\,, && (34c) \end{aligned}$$

where we have used the identity $p_0^2 = (p_0 - 4\pi^2)/\eta$. Boundary condition $\overline{y}_2'(1) = 0$ requires $c_\beta = 2\, c_\gamma$, that is:

$$\omega_1^2 = \frac{2\pi^2}{3\eta}\ \frac{1 - \eta\left(22\pi^2 + p_0\right) + 4\pi^2\eta^2\left(16\pi^2 + 5p_0\right)}{1 - \eta\,(16\pi^2 + p_0) + 4\pi^2\eta^2\,(8\pi^2 + 3p_0)}\,, \tag{35}$$

where we clearly see the singular $\eta \to 0$ limit. Finally we express $\omega = \omega_1\epsilon + O(\epsilon^2)$ as a function of the height of the arch at equilibrium: $y_e(1/2)$. From (22c) we obtain $y_e(1/2) = 4\pi\epsilon/p_0 + O(\epsilon^3)$, which gives us a measure of ϵ. Hence we have

$$\omega = \frac{p_0\,\omega_1}{4\pi}\, y_e(1/2) + O(\epsilon^2)\,. \tag{36}$$

Using (22d) and expanding for small η yields

$$\omega = \sqrt{\frac{2}{3\eta}}\,\pi^2\, y_e(1/2)\,\left[1 + \pi^2\eta + O(\eta^2)\right] + O(y_e^2(1/2))\,. \tag{37}$$

Noting that $\sqrt{2/3}\,\pi^2 \simeq 8.058$, we recover the numerical interpolation given in Eq. 22 of [8]. In Fig. 2 we compare this linear approximation $\omega \simeq 2\pi^2\sqrt{2}\,Y_e(L/2)/h$ with the nonlinear numerical solution of system (15) and we see that it is only valid when the equilibrium height of the arch $Y_e(L/2)$ is less than twice the thickness h.

5.2. Vibrations in the dead loading case

In the dead loading case the solution (22) to the equilibrium problem is the same as in the rigid loading case, but the solution for spatial modes differs and we show that the singularity $1/\eta$ no longer exists. We use the boundary condition $\overline{n}_x(1) = 0$ in (17). To order ϵ^0 the solution is the same as before, given by (26). To order ϵ^1 the transverse mode is also still given by (28), but the solution for the longitudinal mode is now

$$\overline{x}_1(s) = A_0\,\frac{1 - 2\eta p_0}{1 - \eta p_0}\,\frac{\sin 4\pi s - 4\pi s}{4}\,, \tag{38}$$

$$\overline{n}_{x1}(s) = 0\,. \tag{39}$$

We see that $\overline{x}_1(1) \neq 0$, that is the axial displacement at $s = 1$ is no longer fixed. Moreover the $1/\eta$ singularity present in (30b) no longer exists. To order ϵ^2 longitudinal equations and solutions (32) stay the same. For the transverse mode $\overline{y}_2(s)$ the equation has the same structure as (33) but with a different c_β coefficient. Boundary condition $\overline{y}_2'(1) = 0$ here yields the non-singular:

$$\omega_1^2 = \frac{4\pi^4}{3}\ \frac{1 - 2\eta\left(16\pi^2 - p_0\right)}{1 - \eta\,(16\pi^2 + p_0) + 4\pi^2\eta^2\,(8\pi^2 + 3p_0)} \tag{40}$$

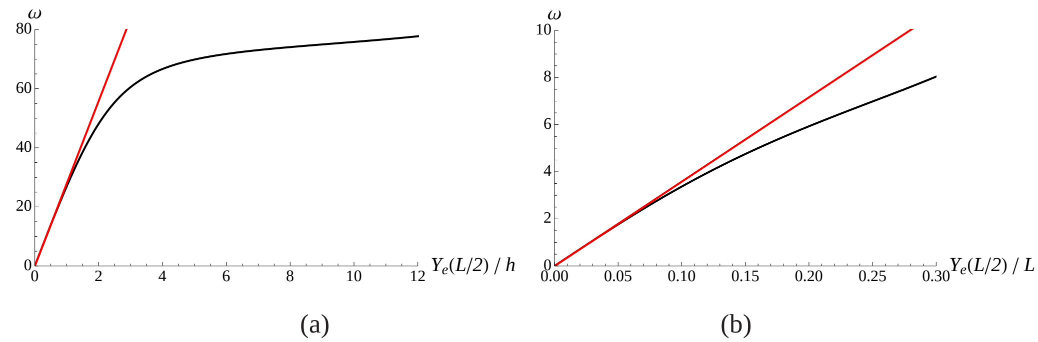

Figure 2: Post-buckling evolution of the first frequency of system (10) as a function of the equilibrium height of the arch $Y_e(L/2)$. The physical frequency is $\Omega = \omega/\tau$ where τ is defined in Section 2. Plain curves (black) have been computed by numerically solving the nonlinear system (15) with boundary conditions (17) and $L = 40\,h$. Straight lines (red) are first order approximations given in Section 5. (Left) Rigid loading case. The equilibrium height of the arch $Y_e(L/2)$ is plotted in h units. The (red) approximation is given by formula (37) and is only valid when the equilibrium height of the arch $Y_e(L/2)$ is less than twice the thickness h. (Right) Dead loading case. The equilibrium height of the arch $Y_e(L/2)$ is plotted in L units. The (red) approximation is given by formula (41). Note that for $L = 40\,h$, $Y_e(L/2)/L = 0.3$ is equivalent to $Y_e(L/2)/h = 12$.

We finally arrive at the expansion

$$\omega = \frac{2\pi^3}{\sqrt{3}}\, y_e(1/2)\left[1 + 2\pi^2\eta + O(\eta^2)\right] + O(y_e^2(1/2)) \tag{41}$$

In Fig. 2 we compare this linear approximation $\omega \simeq \frac{2\pi^3}{\sqrt{3}}\, Y_e(L/2)/L$ with the nonlinear numerical solution of system (15).

6. Discussion

The $1/\eta$ singularity present in the rigid loading case can be analyzed as following. As the rod extremities are strongly held by clamps, the vibrations have to be confined to the rod. Just after buckling the rod is nearly flat and the first mode necessitates extensional deformations to develop. Consequently as the thickness h (or η) is reduced, the system gets stiffer and the mode frequency is rapidly rising. In the limit $\eta \to 0$ the mode ceases to exist at buckling.

In Fig. 3 we plot first modes frequencies as functions of the axial load p_e or axial displacement d_e in both rigid and dead loadings. From (37), (22c), and (22d) in rigid loading we have

$$\omega \simeq \frac{2}{\sqrt{3\eta}}\,\sqrt{p_e - p_0}\,, \tag{42}$$

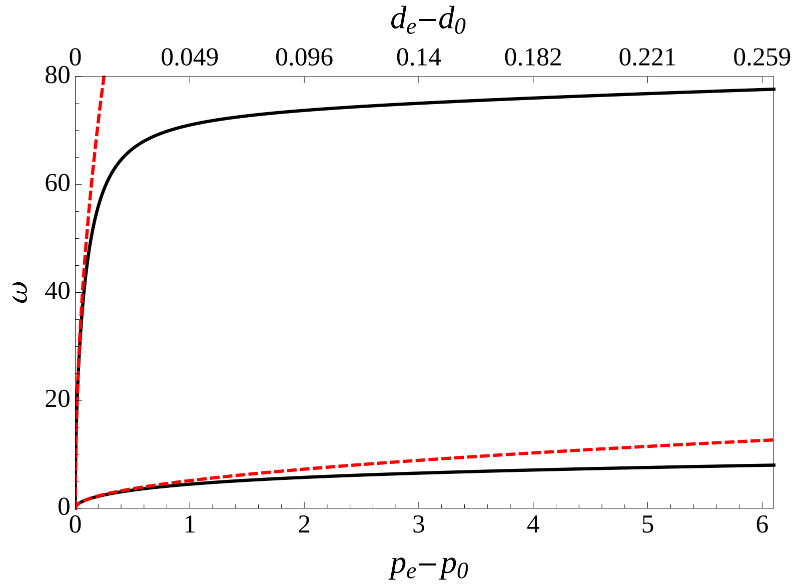

Figure 3: Post-buckling evolution of the first frequency of system (10) as a function of the axial load p_e or axial displacement d_e. The load p_0 and the displacement $d_0 = \eta p_0$ at buckling are used as references. The plain (black) curves have been computed by numerically solving nonlinear system (15) with boundary conditions (17) and $L = 40\,h$, the lower (resp. upper) curve being for the dead (resp. rigid) loading case. Dashed (red) curves are analytic approximations, given by (42) in the rigid loading case and (43) in the dead loading case. The physical frequency is $\Omega = \omega/\tau$ where τ is defined in Section 2. Note that for $L = 40\,h$, $p_e - p_0 = 6$ approximately corresponds to $Y_e(L/2)/h = 12$ or $Y_e(L/2)/L = 0.3$.

and from (41), (22c), and (22d) in dead loading we have

$$\omega \simeq 2\pi \sqrt{2/3}\, \sqrt{p_e - p_0}\,. \tag{43}$$

We see that the frequency in the rigid loading case is much higher that in the dead loading case. This difference can be analyzed as following. As said above, in the rigid loading case the first mode necessitates extensional deformations to develop, resulting in a high frequency when η is small. In the dead loading case axial movement of the right clamp is possible and the first mode is able to develop without having so much to rely on extensional deformations. The system is then comparatively softer and its frequency lower.

7. Conclusion

We have considered an unshearable elastic rod bent in the plane, undergoing flexural and extensional deformations but no twist. We have calculated analytically the post-buckled equilibrium shape of such a rod together with the first vibration mode around this shape. We have studied the dependance of the frequency of this mode with the rod slenderness ratio h/L and we have shown that in the rigid loading case the frequency becomes singular as $h/L \to 0$, while in the dead loading case the singularity does not exist.

Acknowledgements

This publication is based in part upon work supported by Award No. KUK-C1-013-04, made by King Abdullah University of Science and Technology (KAUST) (AG). AG is a Wolfson/Royal Society Merit Award holder. Support from the Royal Society, through the International Exchanges Scheme (grant IE120203), is also acknowledged.

References

References

[1] L. N. Virgin, Vibration of axially loaded structures, Cambridge University Press, 2007.

[2] N. C. Perkins, Planar vibration of an elastica arch: Theory and experiment, Journal of Vibration and Acoustics 112 (1990) 374–379.

[3] J. Casals-Terre, A. Fargas-Marques, A. Shkel, Snap-action bistable micromechanism actuated by nonlinear resonance, Journal of Microelectromechanical Systems 17 (2008) 1082–1093.

[4] Y. Chandra, I. Stanciulescu, L. N. Virgin, T. G. Eason, S. M. Spottswood, A numerical investigation of snap-through in a shallow arch-like model, Journal of Sound and Vibration (2013) –.

[5] J. M. T. Thompson, Stability of elastic structures and their loading devices, Journal of Mechanical Engineering Science 3 (1961) 153–162.

[6] J. M. T. Thompson, Stability predictions through a succession of folds, Philosophical Transactions of the Royal Society of London. Series A, Mathematical and Physical Sciences 292 (1979) 1–23.

[7] S. S. Antman, Nonlinear problems of elasticity, Springer-Verlag, New York, 2nd edition, 2004.

[8] S. Neukirch, J. Frelat, A. Goriely, C. Maurini, Vibrations of post-buckled rods: The singular inextensible limit, Journal of Sound and Vibration 331 (2012) 704 – 720.

[9] M. Potier-Ferry, Fundations of elastic postbuckling theory, in: Buckling and Post-Buckling, volume 288 of *Lectures Notes in Physics*, Springer, 1985, pp. 1–83.

RECENT REPORTS

13/09	Mathematical analysis of a model for the growth of the bovine corpus luteum	Prokopiou Byrne Jeffrey Robinson Mann Owen
13/10	Capillary deformations of bendable films	Schroll Adda-Bedia Cerda Huang Menon Russell Toga Vella Davidovitch
13/11	Twist and stretch of helices: All you need is Love	Đuričković Goriely Maddocks
13/12	Switch on, switch off: stiction in nanoelectromechanical switches	Wagner Vella
13/13	Pinning, de-pinning and re-pinning of a slowly varying rivulet	Paterson Wilson Duffy
13/14	Travelling-wave similarity solutions for a steadily translating slender dry patch in a thin fluid film	Yatim Duffy Wilson
13/15	A stochastic model for early placental development	Cotter Klika Kimpton Collins Heazell
13/16	Experimentally-calibrated population of models predicts and explains inter-subject variability in cardiac cellular electrophysiology	Britton Bueno-Orovio Van Ammel Lu Towart Gallacher Rodriguez
13/17	Elastometry of deflated capsules elastic moduli from shape and wrinkle analysis	Knoche Vella Aumaitre Degen Rehage Cicuta Kierfeld
13/18	The effect of a concentration-dependent viscosity on particle transport in a channel flow with porous walls	Herterich Griffiths Field Vella

13/25	Growth-induced axial buckling of a slender elastic filament embedded in an isotropic elastic matrix	O'Keeffe Moulton Waters Goriely
13/26	The counterbend phenomenon: a generic property of the axoneme and cross-linked filament bundles	Gadêlha Gaffney Goriely
13/27	A well-posedness framework for inpainting based on coherence transport	März
13/28	Minimizing synchronizations in sparse iterative solvers for distributed supercomputers	Zhu Gu Liu
13/29	Computational probabilistic quantification of pro-arrhythmic risk from scar and left-to-right heterogeneity in the human ventricles	Wallman Bueno-Orovio Rodriguez
13/30	Population of human ventricular cell models calibrated with in vivo measurements unravels ionic mechanisms of cardiac alternans	Zhou Bueno-Orovio Orini Hanson Haywood Taggart Lambiase Burrage Rodriguez
13/31	On the eigenvalues and eigenvectors of nonsymmetric saddle point matrices preconditioned by block triangular matrices	Pestana

Copies of these, and any other OCCAM reports can be obtained from:

Oxford Centre for Collaborative Applied Mathematics
Mathematical Institute
24 - 29 St Giles'
Oxford
OX1 3LB
England
www.maths.ox.ac.uk/occam